

Strontium isotopic evidence for supercontinental breakup and formation in the Riphean: Western margin of the Siberian craton

E. M. Khabarov, V. A. Ponomarchuk, and I. P. Morozova

Joint Institute of Geology, Geophysics, and Mineralogy, Russian Academy of Sciences, Siberian Division, Novosibirsk

Abstract. Sr isotopic composition in carbonate rocks of the Baikit anteklise and Yenisei Ridge, western margin of the Siberian craton, has been analyzed. These rocks were formed between 1500–1450 and 850 Ma. Carbonate deposits of the Baikit anteklise are featured by low Sr isotopic ratios that increase gradually from 0.70404 to 0.7052 up the stratigraphy. Riphean carbonate rocks of the Yenisei Ridge exhibit a wide scatter of $^{87}\text{Sr}/^{86}\text{Sr}$ (0.7050–0.7095 or higher). High Sr isotopic ratios are coupled chiefly with considerable postdepositional changes of the rocks. Comparing $^{87}\text{Sr}/^{86}\text{Sr}$ trends and rocks assemblages formed at different positions of the relative sea-level shows that lows on the $^{87}\text{Sr}/^{86}\text{Sr}$ curve correlate well with transgressions and relative sea level highstands, while high Sr isotopic ratios correspond to sea-level drops.

Introduction

By now, ample data on the initial Sr isotope composition of marine carbonates have been acquired, and $^{87}\text{Sr}/^{86}\text{Sr}$ variations through geologic history have been shown to reflect the global balance of matter supplied to the ocean chiefly in the form of two fluxes: mantle-derived, with low $^{87}\text{Sr}/^{86}\text{Sr}$ values, and continental, with higher Sr isotope ratios. Importantly, Sr isotopic composition is relatively constant across the world ocean at any given point along the geologic time scale, and it varies in keeping with the balance just mentioned. The established regularities in the behavior of Sr isotopes are used broadly to assess events of various scales in the upper geospheres and to tackle stratigraphic problems [Faure, 1986; Gorokhov *et al.*, 1995]. Establishing Sr isotopic composition is crucial in pinpointing the episodes of supercontinental breakup and formation, because these processes are accompanied by global changes in the mantle/continent Sr balance in the ocean. The paper provides data from our study of Sr isotopic composition in carbonate

rocks of the Baikit anteklise, western Siberian craton (ca. 100 samples), and of the Yenisei Ridge (ca. 60 samples), that were formed between 1500–1450 and 850 Ma.

Geologic Framework and Stratigraphy

The Baikit anteklise sits on the west of the Siberian craton, and it is viewed as a vast oil and gas bearing structure, where productive strata are of Riphean age [Kontorovich *et al.*, 1996]. The Riphean structural level of the Baikit anteklise exhibits several blocks with varying degree of dislocation and numerous faults, not infrequently with separation in excess of 1 km, so that different stratigraphic horizons are exposed at the pre-Vendian erosion surface. The Riphean stratigraphic pile is divisible into several sequences, in ascending order (Figure 1): Zelendukonsky (quartz and quartz–feldspar sandstones, less frequently gravelstones, conglomerates, and siltstones), Vedreshevsky (greenish gray and dark gray mudstones with intercalations and horizons of siltstones and, sporadically, of limestones and dolomites), Madrinsky (dark gray mudstones, often silty, with thin intercalations and members of clayey dolomites and siltstones), Yurubchensky (gray and dark gray stromatolite dolomites and lumpy intraclastic dolomites with intercalations and members of quartz sandstones and sandy dolomites, espe-

Copyright 2002 by the Russian Journal of Earth Sciences.

Paper number TJE02096.

ISSN: 1681–1208 (online)

The online version of this paper was published 16 July 2002.

URL: <http://rjes.wdcb.ru/v04/tje02096/tje02096.htm>

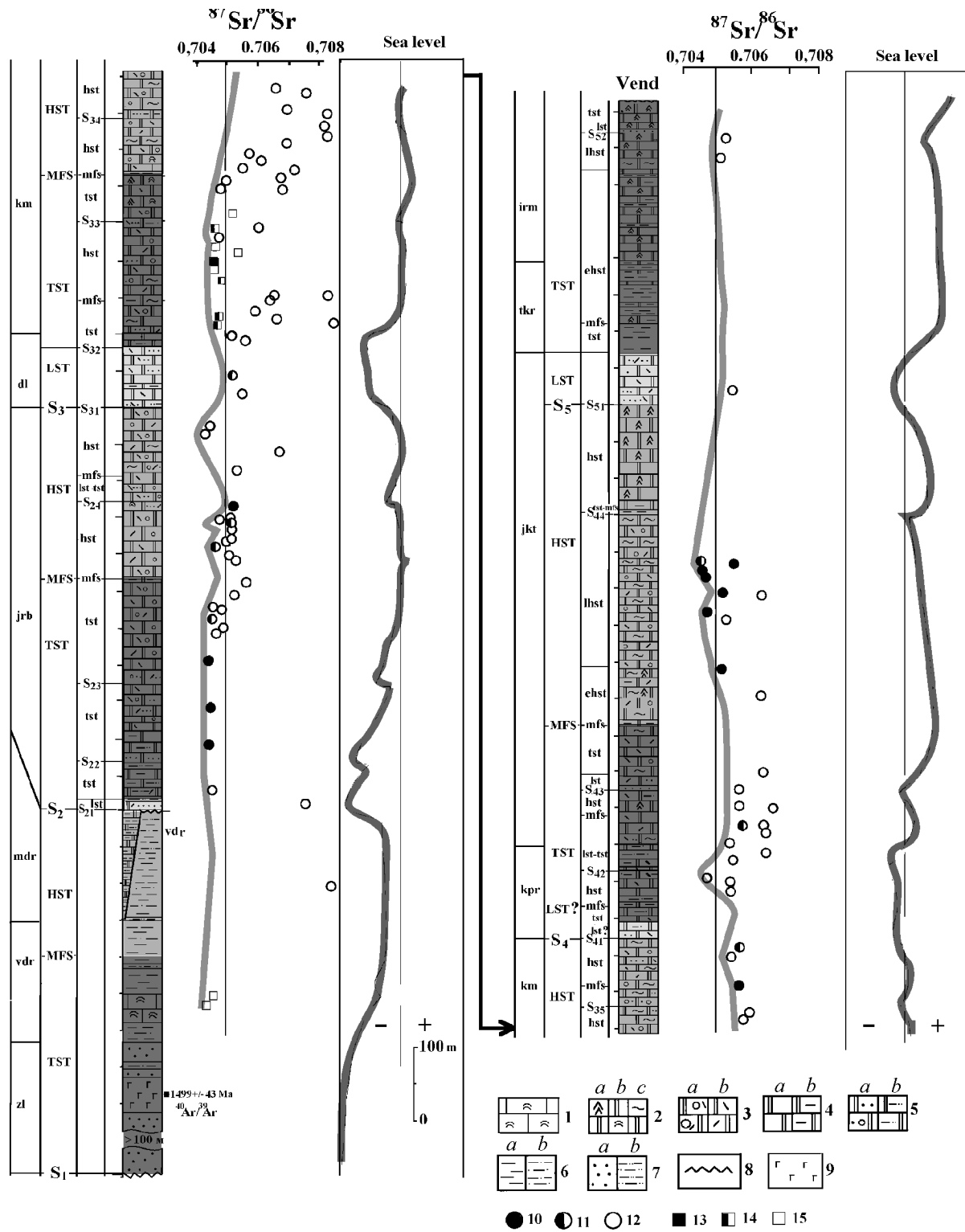


Figure 1. Sea-level variations and Sr isotopic composition in the Riphean basin of the Baikit antecline, Siberian craton.

1 – stromatolite limestones; 2–5 – dolomites: 2 – stromatolitic, from (a) columnar conophytic, (b) columnar branching, and (c) algal laminated stromatolites; 3 – granular oolitic lumpy pisolitic (a), oolitic lumpy intraclastic (b); 4 – (a) micritic siltitic, partly recrystallized, and (b) clayey; 5 – (a) sandy and sand-bearing, (b) silty and silt-bearing; 6 – mudstones (a) and silty mudstones (b); 7 – sandstones (a)

cially in the lower part), Dolgoktinsky (mudstones and siltstones with intercalations and members of dolomites and siliciclastic sandstones), Kuyumbinsky (greenish gray and dark gray stromatolite dolomites and lumpy pisolitic intraclastic dolomites (occasionally limestones) with sporadic intercalations and members of silty sandstones and mudstones), Kopchersky (gray, dark gray, and greenish gray silty mudstones, dolomites, siltstones), Yuktensky (light gray, with greenish and cream hue, stromatolite dolomites and lumpy pisolitic intraclastic dolomites with members of siliciclastic sandstones in the lower part), Tokursky (greenish gray mudstones intercalated by dolomites), and Iremekensky (stromatolite dolomites with mudstone horizons). Laterally, the assemblages are variable in terms of thickness and lithology.

Stratigraphic position of the pre-Vendian section is open to discussion. From general geologic framework, it follows that these deposits were formed prior to the Early Baikalian collision, manifested extensively on the adjoining Yenisei Ridge—i.e., no later than 800–850 Ma; however, the timing of inception of the Baikit basin remains poorly constrained. Some workers [Khomentovskiy and Nagovitsin, 1998; Kraevskiy and Pustynnikov, 1991] believe that the Baikit anticline contains no deposits older than 1100–1150 Ma, while others assign the pre-Vendian deposits to the Paleoproterozoic [Vinogradov *et al.*, 1998]. We allow for broad development of Lower–Middle Riphean rocks in the stratigraphy [Khabarov *et al.*, 1996, 1998]. K/Ar dating on “pure” stromatolite-dominated carbonate rocks, where potassium is associated chiefly with microinclusions of hydromicaceous clay material in crystal lattice defects of carbonate minerals, shows Vedreshevskiy stromatolite limestones to be no younger than 1400 Ma (1390±30 and 1464±90 (1 σ) Ma). Deposits of the upper Yurubchensky Sequence have K/Ar age of ca. 1270 Ma (1290±36 and 1220±95 (1 σ) Ma); Kopchersky, ca. 1100 Ma; and the youngest rocks (upper Yuktensky and Iremekensky Sequences), 1015±40 and 1030±30 (1 σ) Ma. Unfortunately, these age determinations are featured by large error margins; but, nonetheless, they permit constraining the likely minimum age of the carbonate assemblages.

Within the Baikit anticline, Holes Yu-30 and K-5 have penetrated syndepositional doleritic sills, documented among sandstones at the base of the Riphean sequence (Hole Yu-30) and at the faulted boundary between Riphean strata and granite–gneiss basement. Petrographically and geochemically, these rocks are classed as subalkaline dolerites with elevated proportions of Ti-magnetite and Ti-augite. Minor amounts of biotite, which accommodates the bulk of potassium in the rocks, are observable. Earlier, we obtained $^{40}\text{Ar}/^{39}\text{Ar}$ determinations of dolerites from Hole

Yu-30, showing their age to be no younger than 1430±14 (2 σ) and, in all likelihood, no older than 1570±27 (2 σ) Ma [Khabarov *et al.*, 1999]. To refine the timing of emplacement of dolerite sills, additional measurements were made on samples from both holes, Yu-30 and K-5. On K-5 and Yu-30 age spectra, relatively smooth segments account for no more than 25–30% of the entire argon released. Plateau ages for the two samples are similar: 1502±15 Ma for K-5 and 1499±43 Ma for Yu-30. From Hole K-5, two more dolerite samples have been dated. One yields temperature spectra differing but little from the one just mentioned. The plateau age (35% of ^{39}Ar released) equals 1496±9 Ma [Ponomarchuk and Khabarov, 2001]. These data agree well with the results of analysis of magmatism within the Yenisei Ridge. In its eastern zones, mafic volcanism emplacement occurred only during rifting pulses in Early Riphean time. Later episodes of Riphean volcanism have only been recorded in western zones and are not encountered east of the Kaitbinsky zone. Therefore, isotope geochronologic data suggest that the pre-Vendian stratigraphy of the Baikit anticline is clearly dominated by Lower–Middle Riphean rocks. The Riphean basin was incepted no later than 1500–1550 Ma. The age of the oldest limestones studied, Vedreshevskiy, is apparently at least 1400–1450 Ma, and of carbonate deposits from the uppermost part of the pre-Vendian pile, ca. 1000–950 Ma. Quite possibly, however, the obtained K/Ar dates, especially for the upper horizons of the Baikit section, have been reset, and their depositional age is older than 1100 Ma.

The Yenisei Ridge is a complex fold-and-thrust structure formed mainly in the course of the early Baikalian collision (ca. 850 Ma) and modified during subsequent geologic events. The Riphean is represented by a thick (10–12 km) assemblage of laterally variable siliciclastic, carbonate, and volcano-sedimentary rocks. The latter gravitate toward the western zones. The section is divided into four Groups, in ascending order: Teisky, Sukhopitsky, Tungusiksky, and Osl'yansky, overlain with angular unconformity by Upper Proterozoic (Baikalian and Vendian) sequences (Figure 2). The Sukhopitsky Group is divided into six formations: Kordinsky terrigenous–carbonate (up to 700 m thick), Gorbilovskiy green-colored fine siliciclastic (750–900 m), Udereiskiy fine siliciclastic with a clayey limestone member in its middle part (up to 1200 m), Pogoryuiskiy clay–silt–sand (up to 750 m), Kartochki limestone–clay (up to 150 m), and Aladinsky dolomite (up to 500 m). The Tungusiksky Group in the Kamensky zone is divided into five Formations: Krasnogorsky siliciclastic (60–140 m), Dzhursky carbonate (up to 400 m), Shuntarsky dark colored carbonate–terrigenous (up to 1000 m), Sery Klyuch carbonate (up to 600 m), and Dadyktinsky carbonate–terrigenous (Rybinsky

and siltstones (b); 8 – regional hiatus; 9 – diabase; 10–12 – dolomites: 10 – least altered, 11 – moderately altered, 12 – altered; 13–15 – limestones: 13 – least altered, 14 – moderately altered, 15 – altered. Sequences: Zl = Zelendukonsky, Vdr = Vedreshevskiy, Mdr = Madrinsky, Yrb = Yurubchensky, Dl = Dolgoktinsky, Km = Kuyumbinsky, Kp = Kopchersky, Yukt = Yuktensky, Tkr = Tokursky, Irm = Iremekensky. Sequence boundaries of 2nd (S) and 3rd (s) order. Sedimentary system tracts: of sea-level lowstand of 2nd (LST) and 3rd (lst) order; transgressive, of 2nd (TST) and 3rd (tst) order; of sea-level highstand of 2nd (HST) and 3rd (hst) order; early stage (ehst) and late stage (lhst) of 3rd order sea-level highstand. Maximum flooding surfaces of 2nd (MFS) and 3rd (mfs) order.

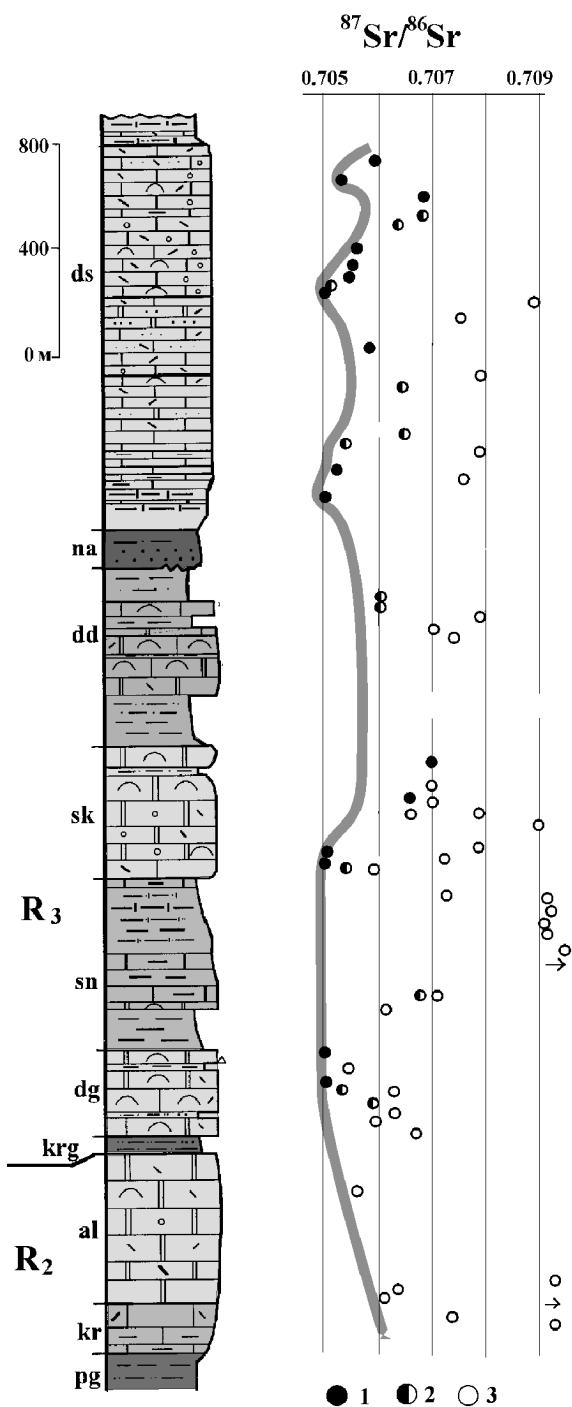


Figure 2. Variations of Sr isotopic composition in the Riphian basin of the Yenisei Ridge.

1–3 – carbonate rocks: 1 – least altered, 2 – moderately altered, and 3 – altered. Formations: Pg = Pogoryuiski, Kr = Kartochki, Al = Aladinsky, Krg = Krasnogorsky, Dg = Dzhursky, Sn = Shuntarsky, Sk = Sery Klyuch, Dd = Dadyktinsky, LA = Lower Angara, Ds = Dashkinsky. Other symbols, as in Figure 1.

and Mokrinsky Formations in the Gorbilovsky zone) (up to 600 m). At the base of the Osl'yansky Group, there occurs conformably, albeit in places erosionally, the siliciclastic Lower Angara Formation (up to 350 m), overlain by the limestone-dominated Dashkinsky Formation (up to 1500 m).

Glauconite K–Ar dates of ca. 1100 Ma have been reported from the Pogoryuiski Formation, from the top of the Krasnogorsky Formation (1007 ± 15 Ma), and from the base of the Dzhursky Formation (924 ± 40 Ma). Also available are age determinations (ca. 850 Ma) from granites cutting through the Tunguskiy Group deposits [Shenfil, 1991, and references therein]. According to these data, carbonate rocks from the upper part of the Sukhopitsky Group are no older than 1100 and no younger than 1000 Ma, while those from the Tunguskiy and Osl'yansky Groups are constrained between 1000 and 850 Ma.

Analytical Methods

Estimating variations of Sr isotopic composition in marine basins requires samples in which Sr was, during sediment deposition, in isotopic equilibrium with sea-water Sr, and which remained a closed system with respect to Sr subsequently. For this reason, we selected least recrystallized samples with minimum silicate component. Precise location of samples in surface exposures on the Yenisei Ridge and in drillholes in the Baikit anticline is given in [Khabarov *et al.*, 1999, 2002]. Alteration degree of carbonate rocks was assessed from petrographic, geochemical (Mn/Sr, Fe/Sr, Rb/Sr), and isotope geochemical data ($\delta^{18}\text{O}$ and the difference ($\Delta\delta^{13}\text{C}$) between $\delta^{13}\text{C}_{\text{carb.}}$ and $\delta^{13}\text{C}_{\text{org.}}$). Meanwhile, carbonate rocks, even slightly recrystallized, represent a heterogeneous system recording the outcome of a complex interplay of both syn- and postdepositional processes; accordingly, each component of such a system may have its distinctive Sr isotope ratios. For this reason, within each sample, fragments were identified with distinctive macro- and microscopic characteristics, which were then studied separately. To identify the most reliable initial $^{87}\text{Sr}/^{86}\text{Sr}$ ratios, stage-by-stage decomposition of limestones and dolomites was also applied in development of the approach of [Gorokhov *et al.*, 1995]. During the first stage, samples (or their fragments) were treated with 0.01N HCl, and then 2–4 successive fractions obtained from dissolution of carbonates in 0.1N HCl were collected. The fractions of dissolved carbonate (usually second and, less frequently, the rest of the fractions) in which $^{87}\text{Sr}/^{86}\text{Sr}$, elemental ratios such as Mn/Sr, Fe/Sr, and Rb/Sr, and Rb contents were the lowest were considered to be the most suitable. All the reagents used were put to repeated purification. Chemical processing was carried out in a special room using quartz and fluoroplastic vessels.

Sr isotopic composition was studied in the dissolved fraction, evaporated until dry, using chromatographic extraction of Sr and Rb isotopes. Sr and Rb isotopic compositions were measured on a MI 1201-T mass spectrometer using rhenium filaments. Instrument performance stability was controlled using a VNIIM SrCO_3 standard, whose composition remained within 0.70811 ± 15 in the course of measure-

ments. Rb background was 7×10^{-10} g, and Sr background, 1×10^{-9} g. Carbon and oxygen isotopic compositions were measured on a Finnigan D mass spectrometer (with a 0.1‰ error margin), and Ca, Mg, Fe, Mn in soluble fraction of carbonate rocks were measured by atomic absorption on a SP9 PI UNIKAM installation (with an error margin no greater than 5%).

Dolerite samples for $^{40}\text{Ar}/^{39}\text{Ar}$ dating collected from drill-cores were rinsed repeatedly in distilled water and 1N HNO_3 to remove drilling mud and carbonate microadmixture. Charges of 50–80 mg from sample fragments in the form of 0.1–0.25 mm particles were irradiated on a nuclear reactor following the procedure required in Ar–Ar studies.

While constructing the variation curve of Sr isotopic composition for pre-Vendian carbonate deposits of the Baikit antecline and Yenisei Ridge, the lowest $^{87}\text{Sr}/^{86}\text{Sr}$ ratios obtained from samples or their fragments were taken into account, because secondary processes, as a rule, increase initial values.

Results and Discussion

Postdepositional Alteration of Carbonate Rocks

Estimating the degree of postdepositional alteration of rocks is viewed as a necessary step in isotope geochemical studies [Asmerom *et al.*, 1991; Brand and Veizer, 1981; Derry *et al.*, 1992; Gorokhov *et al.*, 1995; Veizer, 1983; and others].

Petrographic characteristics of the rocks. Most samples from the deposits of the Baikit antecline are represented by dolomites that formed through the earliest diagenetic replacement of calcareous sediment and vigorous isotope exchange with sea water. The lower part of the carbonate section contains abundant micromatolites and laminites with well-preserved fibrous textures. Because of their crystallographic peculiarities, these textures indicate that the original sediment was most likely represented by aragonite [Grotzinger and Read, 1983]. On the Yenisei Ridge, samples were collected mainly from limestones.

The carbonate rocks exhibit varying degree of recrystallization. Limestones are usually only slightly recrystallized, retaining a significant proportion of primary micritic material. Primary textures are especially well preserved in limestones of the Dashkinsky Formation of the Osl'yansky Group. Weakly recrystallized dolomites also largely preserve the micritic component in grains and matrix. In the more strongly recrystallized varieties, coarsely crystalline dolomite is developed in patches and veinlets affecting grains and intergrain spaces. Rocks are observed where only relics of primary sedimentary texture survive. Under pervasive recrystallization, primary texture is completely obliterated.

Available data show that recrystallization does not expressly control Sr isotopic composition in the studied rocks. Thus, strongly recrystallized dolomite samples (Hole Yu-30) have yielded very low (below 0.7050) $^{87}\text{Sr}/^{86}\text{Sr}$ ratios, which

are apparently close to initial. Meanwhile, in samples with numerous microcaverns, related genetically to microjoints and stylolites filled with Fe-dolomite, original isotopic systems have most likely been reset.

Geochemical and isotope geochemical characteristics of the rocks. To estimate the degree of alteration of samples and of the $^{87}\text{Sr}/^{86}\text{Sr}$ values obtained, widely applied is a set of geochemical and isotope geochemical criteria: Mn, Fe, and Rb contents; Mn/Sr, Fe/Sr, and Rb/Sr ratios; $\delta^{18}\text{O}$ values; and the presence or absence of covariation between $\delta^{18}\text{O}$ and $^{87}\text{Sr}/^{86}\text{Sr}$. They are used because during post-depositional alteration, carbonate rocks are commonly enriched in Mn, Fe, and Rb and depleted in Sr. In the process, $\delta^{18}\text{O}$ values decrease [Brand and Veizer, 1981; Knoll *et al.*, 1995; Sochava *et al.*, 1996; Veizer, 1983; and others].

Analyzing geochemical characteristics of the samples and their fragments and the covariation between $^{87}\text{Sr}/^{86}\text{Sr}$ and Mn/Sr, Fe/Sr, Rb/Sr values has shown that in terms of Mn/Sr and Fe/Sr ratios, all the dolomite samples, even using moderately rigorous criteria adopted for limestones, fall with clearly altered rocks, and it is only in terms of Rb/Sr ratios that some of the samples can be classed as unaltered. Meanwhile, geochemical characteristics of the dolomites are overall nonuniform, with Mn/Sr, Fe/Sr, and Rb/Sr ratios ranging widely and correlating poorly with the initial $^{87}\text{Sr}/^{86}\text{Sr}$ values (Tables 1, 2).

The studied dolomites are low in Sr (12.8–77 ppm; mostly, below 40 ppm). Similar Sr contents are recorded in dolomites from other regions and are sharply dissimilar from those in limestones, where Sr contents are no lower than 100 ppm and occasionally above 1000 ppm. The higher Sr contents of limestones are due to the fact that ion radii are appreciably different for Sr and Mg, with the result that Sr enters calcite lattice more readily than dolomite lattice [Veizer, 1983]. For this very reason, dolomites are in many cases enriched in Mn and Fe [Veizer *et al.*, 1992a]. Hence, geochemical criteria may reflect, on the one hand, actual postdepositional alteration of dolomites, and, on the other, their crystallochemical features, while Sr isotopic composition may remain close to initial. Therefore, in assessing the degree of alteration of dolomite, in contrast to limestones, we used less rigorous elemental ratios: Mn/Sr < 2.5, Fe/Sr < 60, Rb/Sr < 0.005. Besides, we took into account the contents of Mn (< 200 ppm), Fe (< 2000 ppm), and Rb (chiefly, < 0.5 ppm). For limestone samples, we used more rigorous elemental ratios: Mn/Sr < 0.5, Fe/Sr < 5.0, Rb/Sr < 0.001.

In the studied samples, $\delta^{18}\text{O}$ is usually above -5‰ , and it is only in limestones that it drops to -10 – -12‰ . The lack of an express correlation between $\delta^{18}\text{O}$ and $^{87}\text{Sr}/^{86}\text{Sr}$ values suggests that the samples are altered weakly. In this work, samples with $\delta^{18}\text{O}$ below -7‰ (for limestones, below -10‰) are classed as being relatively altered and may record $^{87}\text{Sr}/^{86}\text{Sr}$ values departing from initial ones. Between the “least altered” and “altered” samples, one can place a group of “moderately altered” ones, some parameters of which (usually, good Rb/Sr characteristics) stay within adopted boundary values, while others (especially, Fe/Sr ratios) overstep the boundary values just slightly.

Table 1. Chemical and isotopic compositions of pre-Vendian carbonate rocks of the Baikit antecline

Sample	Sequence	Mn, ppm	Fe, ppm	Mg/Ca	Mn/Sr	Fe/Sr	Rb/Sr	Rb, ppm	Sr, ppm	$^{87}\text{Rb}/^{86}\text{Sr}$	$^{87}\text{Sr}/^{86}\text{Sr}$, measured	$^{87}\text{Sr}/^{86}\text{Sr}$, initial	$\delta^{18}\text{O}$ ‰, PDB
1.30.92	Vdr	888.	427.	0.014	10.1	4.8	0.0030	0.277	88.2	0.0090	0.70417	0.70404	-6.0
1.29.92	Vdr	244.	717.	0.016	1.7	4.9	0.0025	0.369	146.1	0.0073	0.70459	0.70448	-7.2
1.85.91	Mdr	72.	2756.	0.620	3.6	134.0	0.0055	0.108	19.5	0.0159	0.70468	0.70445	-3.6
1.22.92	Yrb	88.	415.	0.610	2.2	10.4	0.0009	0.038	39.7	0.0027	0.70440	0.70436	-4.1
12.22.92	Yrb	104.	1920.	0.512	2.2	41.3	0.0009	0.044	46.4	0.0026	0.70475	0.70474	-2.1
12.21.92	Yrb	120.	2610.	0.522	2.3	50.0	0.0009	0.048	52.1	0.0027	0.70422	0.70421	-2.5
1.79.91	Yrb	93.	845.	0.590	3.1	27.9	0.0034	0.112	30.2	0.0109	0.70468	0.70452	-2.9
1.13.92	Yrb	91.	2061.	0.580	2.9	66.7	0.0010	0.051	30.9	0.0133	0.70503	0.70484	-4.2
12.5.92	Yrb	132.	2541.	0.515	3.5	68.5	0.0013	0.050	37.1	0.0035	0.70491	0.70490	-2.6
12.1.92	Yrb	100.	2430.	0.531	2.2	52.9	0.0039	0.182	45.9	0.0114	0.70516	0.70510	-2.5
1.10.92	Yrb	81.	533.	0.670	4.5	30.7	0.0050	0.094	18.0	0.0015	0.70433	0.70430	-5.2
B1.14.97	DI	122.	1180.	0.403	4.0	36.2	0.0060	0.219	32.6	0.0206	0.70510	0.70507	-2.1
K12.129	Kmb	47.	2222.	0.098	0.3	12.2	0.0013	0.300	181.7	0.0047	0.70443	0.70442	-2.3
K12.126	Kmb	69.	1408.	0.062	0.4	8.7	0.0017	0.280	160.7	0.0050	0.70461	0.70460	-2.3
K12.111	Kmb	64.	1041.	0.069	0.2	3.7	0.0025	0.720	281.8	0.0074	0.70489	0.70488	-2.6
21.17.92	Kmb	23.	889.	0.009	0.1	4.0	0.0009	0.216	218.8	0.0028	0.70453	0.70452	-5.5
K12.101	Kmb	62.	1679.	0.055	0.4	12.3	0.0016	0.230	136.7	0.0047	0.70471	0.70470	-2.9
21.16.92	Kmb	118.	830.	0.012	0.8	5.6	0.0017	0.251	146.9	0.0049	0.70461	0.70460	-3.9
1.62.91	Kmb	67.	661.	0.620	1.4	14.4	0.0035	0.182	48.4	0.0103	0.70554	0.70539	-2.7
2.43.91	Kmb	100.	800.	0.570	2.8	22.4	0.0009	0.034	35.6	0.0029	0.70573	0.70571	-4.4
3.11.92	Ykt	70.	3160.	0.518	2.0	92.4	0.0059	0.203	34.2	0.0171	0.70601	0.70576	-2.1
1.49.91	Ykt	27.	384.	0.570	1.4	20.0	0.0020	0.042	19.2	0.0065	0.70518	0.70509	-4.2
1.43.91	Ykt	54.	382.	0.540	1.8	12.7	0.0005	0.016	30.1	0.0014	0.70460	0.70458	-2.8
1.29.91	Ykt	52.	509.	0.530	2.1	21.0	0.0030	0.076	24.2	0.0087	0.70553	0.70521	-3.2
1.22.91	Ykt	63.	885.	0.570	1.0	14.0	0.0007	0.094	63.0	0.0044	0.70478	0.70472	-4.2
1.17.91	Ykt	75.	1085.	0.610	2.5	36.1	0.0010	0.038	30.0	0.0035	0.70468	0.70463	-3.9
1.8.91	Ykt	100.	1370.	0.540	2.0	27.5	0.0010	0.067	49.8	0.0064	0.70570	0.70561	-2.2
2.8.91	Irm	330.	2771.	0.500	6.5	54.8	0.0040	0.241	50.6	0.0137	0.70523	0.70503	-5.9
2.5.91	Irm	401.	2450.	0.420	8.3	50.8	0.0030	0.174	48.2	0.0100	0.70535	0.70520	-4.1

Sequences: Vdr – Vedreshevsky, Mdr – Madrinsky, Yrb – Yurubchensky, DI – Dolgoktinsky, Kmb – Kuyumbinsky, Yrt – Yuktensky, Irm – Iremekensky. Data listed are from the least to moderately altered samples (except for those from the Vedreshevsky, Madrinsky, and Iremekensky Sequences). For stratigraphic position of samples, see Figure 1. Sample location and the correlation of drilled sections are given in [Khabarov *et al.*, 2002].

Variations of Initial Sr Isotopic Composition

In plotting the variation curve of Sr isotopic composition in pre-Vendian carbonate deposits of the Baikit antecline and Yenisei Ridge, we took into account the lowest $^{87}\text{Sr}/^{86}\text{Sr}$ ratios obtained from samples or their fragments, because deuteric processes, as a rule, increase initial values. Note that geologic data rule out the likelihood of postdepositional processes that might have depressed Sr isotope ratios (e.g., isotope exchange with interlayered oceanic mafites with low $^{87}\text{Sr}/^{86}\text{Sr}$ ratios). At the same time, the primary nature of positive $^{87}\text{Sr}/^{86}\text{Sr}$ anomalies is far from being evident, because using the adopted geochemical criteria, samples from these intervals are mainly classed as altered, with likely resetting of Rb/Sr and Sr/Sr isotope systems through isotope exchange between carbonate rocks and fine siliciclastic deposits. The available data, however, suggest that ra-

diogenic Sr contamination of carbonates took place primarily in clayey and clayey silty carbonate rocks, and it often eludes recording even in thinly interbedded “pure” dolomites and mudstones. Within positive $^{87}\text{Sr}/^{86}\text{Sr}$ anomalies, samples are recorded not infrequently that should be classed as weakly altered, based on geochemical criteria.

Let us address variations of Sr isotopic composition in the studied sections (Figures 1, 2). Overall, carbonate deposits of the Baikit antecline are featured by very low Sr isotope ratios. The Vedreshevsky Sequence exhibits low $^{87}\text{Sr}/^{86}\text{Sr}$ (0.70404–0.7048) values, which are also recorded in the Madrinsky Sequence, although in its lower portion these ratios may be higher. The Yurubchensky Sequence displays three intervals. The lower has initial $^{87}\text{Sr}/^{86}\text{Sr}$ ratios of 0.70421–0.70465; the middle, up to 0.7050; then, a descending trend (as low as 0.7043–0.7041?) follows. This trend gives way to an ascending one (up to 0.70507), which persists into the Dolgoktinsky Sequence. In the lower part of the

Table 2. Chemical and isotopic compositions of Riphean carbonate rocks from eastern zones of the Yenisei Ridge

Sample	Height above the base of Formation, m	Mn, pmm	Fe, pmm	Mg/Ca	Mn/Sr	Fe/Sr	Rb/Sr	Rb, pmm	Sr, pmm	$^{87}\text{Rb}/^{86}\text{Sr}$	$^{87}\text{Sr}/^{86}\text{Sr}$ measured	$^{87}\text{Sr}/^{86}\text{Sr}$ initial	$\delta^{18}\text{O}$ ‰, PDB
1	2	3	4	5	6	7	8	9	10	11	12	13	14
pn-1	400?	304.	3617.	0.004	1.9	22.3	0.0017	0.314	180.6	0.0050	0.71000	0.70989	-11.0
kd-2	120	2440.	45250.	0.498	11.3	211.0	0.1530	32.90	214.4	0.4437	0.74150	0.73238	-7.7
kd-3	134	3810.	22290.	0.506	17.7	164.0	0.0310	6.990	222.1	0.0912	0.72759	0.72571	-10.4
ss-1	60	1710.	46900.	0.034	3.2	86.9	0.0085	4.640	540.0	0.0278	0.71483	0.71425	-11.9
ss-2	150	473.	1820.	0.019	0.6	4.5	0.0002	0.086	399.1	0.0074	0.70739	0.70728	-9.9
ss-3	250	541.	1473.	0.028	1.1	3.0	0.0017	0.836	482.8	0.0034	0.70627	0.70622	-11.0
ss-4	270	319.	1496.	0.003	1.5	7.0	0.0001	0.033	212.2	0.0007	0.70663	0.70662	-11.7
ss-5	300	1080.	10370.	0.042	4.6	43.9	0.0373	8.820	236.0	0.0549	0.71835	0.71757	-11.5
al-3.12.7	310	90.	2700.	0.297	2.9	88.4	0.0011	0.035	30.6	0.0035	0.70558	0.70553	-3.6
dg-8	78	127.	751.	0.005	0.4	2.7	0.0014	0.398	276.7	0.0033	0.70598	0.70592	-6.4
dg-10	137	77.	875.	0.007	0.5	5.7	0.0003	0.043	153.4	0.0031	0.70547	0.70543	-7.8
dg-11	148	118.	366.	0.034	0.3	1.0	0.0014	0.536	359.4	0.0043	0.70514	0.70508	-7.1
dg-14	320	152.	2060.	0.020	0.3	4.8	0.0010	0.504	430.0	0.0051	0.70518	0.70511	-5.0
sn-4	380	914.	874.	0.004	1.0	0.9	0.0006	0.596	912.0	0.0015	0.70675	0.70673	-6.6
sk-2.1b.7	90	164.	1610.	0.011	0.3	2.6	0.0014	0.932	632.8	0.0042	0.70550	0.70546	-4.5
sk-2.1a.7	110	290.	2040.	0.012	0.4	3.2	0.0012	0.825	635.6	0.0047	0.70509	0.70505	-2.9
sk-16a	140	131.	461.	0.011	0.3	0.9	0.0018	0.890	486.5	0.0016	0.70507	0.70505	-2.9
sk-11	219	43.	642.	0.002	0.3	4.4	0.0002	0.026	145.6	0.0004	0.70656	0.70655	-6.5
sk-13	345	60.	345.	0.011	0.3	1.9	0.0002	0.043	182.1	0.0009	0.70696	0.70695	-6.5
rb-2	440	175.	3610.	0.006	0.2	3.6	0.0008	0.804	996.8	0.0008	0.70611	0.70604	-10.1
rb-3	445	177.	2870.	0.005	0.2	2.7	0.0002	0.214	1070.0	0.0043	0.70627	0.70621	-10.0
ds-1	100	298.	6670.	0.051	0.2	3.8	0.0003	0.590	1750.0	0.0008	0.70514	0.70513	-7.7
ds-6	225	374.	5640.	0.037	0.4	5.0	0.0009	0.924	944.1	0.0023	0.70530	0.70527	-7.2
ds-8	305	644.	1420.	0.008	1.4	3.1	0.0004	0.196	458.0	0.0009	0.70539	0.70538	-6.8
ds-9	350	205.	3570.	0.108	0.5	8.1	0.0009	0.440	440.8	0.0042	0.70671	0.70666	-3.7
ds-11	515	42.	820.	0.016	0.3	5.4	0.0005	0.078	152.0	0.0011	0.70651	0.70650	-6.3
ds-18	625	63.	530.	0.009	0.4	3.9	0.0009	0.123	137.7	0.0018	0.70586	0.70584	-4.7
ds-24	835	42.	957.	0.032	0.2	4.6	0.0010	0.212	206.2	0.0024	0.70502	0.70499	-2.9
ds-25	850	48.	1430.	0.011	0.2	7.6	0.0009	0.187	189.3	0.0022	0.70515	0.70512	-3.1
ds-27	877	36.	670.	0.007	0.2	4.7	0.0002	0.036	142.6	0.0006	0.70559	0.70558	-3.6
ds-28	905	64.	539.	0.008	0.4	3.1	0.0004	0.065	172.5	0.0008	0.70561	0.70560	-6.2
ds-31	961	183.	1050.	0.007	0.5	2.8	0.0002	0.062	383.3	0.0003	0.70564	0.70563	-6.1
ds-33	1075	228.	504.	0.007	0.5	1.2	0.0002	0.086	435.9	0.0005	0.70640	0.70639	-3.0
ds-35	1110	56.	877.	0.024	0.3	4.6	0.0012	0.226	191.1	0.0025	0.70669	0.70666	-8.6
ds-37	1148	51.	355.	0.025	0.4	3.0	0.0005	0.061	132.5	0.0012	0.70669	0.70667	-4.3
ds-39	1235	32.	681.	0.003	0.04	0.9	0.0001	0.092	708.9	0.0003	0.70547	0.70546	-5.4
ds-40	1275	62.	1760.	0.005	0.1	2.9	0.0001	0.064	602.6	0.0002	0.70598	0.70597	-5.2

Formations: pn – Pechenginsky, kd – Kordinsky, ss – Sosnovsky, al – Aladinsky, dg – Dzhursky, sn – Shuntarsky, sk – Sery Klyuch (sk-16a, sk-2. (a, b).7 – samples from the Angara section), rb – Rybinsky (Dadyktinsky), ds – Dashkinsky. Samples are tied to the base of each Formation under study. Data listed are from the least to moderately altered samples (except those from the Pechenginsky, Kordinsky, Sosnovsky, and Aladinsky Formations). Sample location and the correlation of sections are given in [Khabarov *et al.*, 1999].

Kuyumbinsky sequence, low (0.70442–0.70483) $^{87}\text{Sr}/^{86}\text{Sr}$ ratios are recorded, which then increase to 0.70539–0.70545 or, possibly, higher, finally to decrease at the boundary with the Kopchersky Sequence. The descending trend of $^{87}\text{Sr}/^{86}\text{Sr}$ values (as low as 0.7051–0.70445?) continues into the lower part of the latter, to give way to an ascending one, which is traceable into the lower part of the Yuktensky

Sequence, where Sr isotope ratios in moderately altered samples are as high as 0.7054–0.7055. Further on, these ratios decrease smoothly, equaling 0.70455–0.70463 in the middle part of the Yuktensky Sequence. In the upper Yuktensky and in the Iremekensky Sequences, one finds moderately low (0.70503–0.7052), possibly somewhat overstated $^{87}\text{Sr}/^{86}\text{Sr}$ ratios. Generally, Sr isotope ratios increase gradually from

0.70404 to 0.7052 up the stratigraphy. This trend is occasionally modulated by shifts toward higher $^{87}\text{Sr}/^{86}\text{Sr}$ ratios. The highest $^{87}\text{Sr}/^{86}\text{Sr}$ (0.70539) in a weakly altered sample has been recorded from the upper Kuyumbinsky deposits.

Riphean carbonate rocks of the Yenisei Ridge exhibit a wide scatter of $^{87}\text{Sr}/^{86}\text{Sr}$ (0.7050–0.7095 or higher), yet our petrographic, geochemical, and isotope geochemical studies have shown that high Sr isotope ratios are coupled chiefly with considerable postdepositional changes of the rocks (e.g., in samples from the upper part of the Penchenginsky and the base of the Kordinsky Formations) (Table 2). Samples from the Tunguskiy Group (Dzhursky and Sery Klyuch Formations) and Oslvansky Group (Dashkinsky Formation) of the Upper Riphean, which have best preserved the initial Sr isotope signal, record values of 0.7050–0.70515 (Figure 2). However, weakly altered limestone samples from the Sery Klyuch and Dadyktinsky Formations record some relatively high $^{87}\text{Sr}/^{86}\text{Sr}$ ratios (0.7060–0.7069), although a significant positive excursion is unlikely. Elevated values have also been recorded in altered samples from the upper part of the Middle Riphean Sukhopitsky Group.

Geodynamic Implications of the Results Obtained

Based on present-day data on Sr isotopic composition, the $^{87}\text{Sr}/^{86}\text{Sr}$ evolutionary curve in the Proterozoic ocean can be imaged as an Early to Late Proterozoic ascending trend, modified by highs and lows [Asmerom *et al.*, 1991; Brasier and Lindsay, 1998; Derry and Jacobsen, 1988; Derry *et al.*, 1992; Faure, 1986; Gorokhov *et al.*, 1995, 1998; Hall and Veizer, 1996; Kuznetsov *et al.*, 1997, 2000; Mirola and Veizer, 1994; Pokrovsky and Vinogradov, 1991; Semikhatov *et al.*, 1998; Veizer *et al.*, 1992a, 1992b; Vinogradov *et al.*, 1998]. Overall, the $^{87}\text{Sr}/^{86}\text{Sr}$ vs. time curve (Figure 3) demonstrates that low (below 0.705) Sr isotope ratios are recorded between 2500–2300, 2100–1800, and 1500–1200 Ma. High $^{87}\text{Sr}/^{86}\text{Sr}$ values are documented at ca. 2200, 1600, 1100 Ma. Comparing our own Sr isotope composition data with published ones shows that our $^{87}\text{Sr}/^{86}\text{Sr}$ curves for the Baikit antecline and Yenisei Ridge best fit the fragment of the general evolutionary curve between 1450–1500 and 1000–850 Ma (Figure 3), which seemingly agrees with the available isotope ages. At the same time, data from the Baikit basin are at odds with the available world data because of the low $^{87}\text{Sr}/^{86}\text{Sr}$ values within the 1100 Ma positive anomaly. This might be due to the fact that our own K/Ar ages are reset, and depositional age of the upper part of the pre-Vendian section may be older than 1100 Ma. Accordingly, Figure 3 gives two options (A and B) for age assignment of the $^{87}\text{Sr}/^{86}\text{Sr}$ curve for the Baikit basin.

Results obtained for the Lower and Middle Riphean deposits of the Baikit antecline and from elsewhere on the Siberian craton [Gorokhov *et al.*, 1995; Pokrovsky and Vinogradov, 1991; Vinogradov *et al.*, 1994], from the Bashkir anticlinorium [Kuznetsov *et al.*, 2000], and from the Belt Supergroup, North America [Hall and Veizer, 1996] imply that seawater Sr isotope composition at that time was appreciably less radiogenic than assumed formerly [Derry and Jacobsen, 1988; Faure, 1986]. Not only do these results change sig-

nificantly the notion of Sr isotopic composition in the Meso-Proterozoic world ocean, but they also testify to vigorous processes of the breakup of the Early Proterozoic supercontinent and ocean formation as early as the beginning of the Meso-Proterozoic. The low (less than 0.705) Sr isotope ratios, documented over a timespan of more than 250 m.y., are due primarily to rifting and seafloor spreading, involving mantle Sr supply to the ocean. These conclusions agree well with the data on the evolution of the Yenisei [Kontorovich *et al.*, 1996], Grenville [McLelland *et al.*, 1996], Vitim–Patom [Bozhko, 1995; Bukharov *et al.*, 1992; Dobretsov and Bulgatov, 1991; and others], Zambezi [Oliver *et al.*, 1998], and some other Meso-Proterozoic oceans, which closed at the Meso–Neo-Proterozoic transition or were transformed into Neo-Proterozoic to Paleozoic oceans.

The highest Sr isotope ratios (in relatively altered samples, 0.706 or higher) are recorded from the upper Sukhopitsky deposits, dated at ca. 1100 Ma, in good agreement with the available data from the Siberian craton [Bartley *et al.*, 2001; Gorokhov *et al.*, 1995] and from other continents [Derry and Jacobsen, 1988; Faure, 1986]. The increase in Sr isotope ratios correlates to the closure of oceans and formation of a new major continent of Rodinia during the Grenville events [Dalziel *et al.*, 2000; Powell *et al.*, 1993].

Deposits younger than 1060–1040 Ma exhibit $^{87}\text{Sr}/^{86}\text{Sr}$ values declining gradually to 0.7050–0.7051. A similar trend is recorded in the section of the upper-Middle and basal-Upper Riphean on the Turukhansk uplift [Gorokhov *et al.*, 1995], although Sr isotope ratios there do not drop below 0.70522. These data show that the Late Riphean depression on the Sr isotope curve must have been more considerable and protracted than previously believed [Veizer *et al.*, 1983]. The imminence of expanding the inferred timespan of the Late Riphean “mantle event” has been acknowledged by Gorokhov *et al.* [1995]. Geologic data, by and large, are not inconsistent with this eventuality. Thus, at 950–1050 Ma, a pulse of rifting of the African paleocontinent is recorded [Borg, 1988]. Simultaneously, oceanic crust was being generated vigorously in the Arabian–Nubian paleocean [Quirk, 1990]. On the other hand, such low $^{87}\text{Sr}/^{86}\text{Sr}$ ratios are at odds with the long-lasting existence of the supercontinent of Rodinia between 1000 and 750 Ma [Dalziel *et al.*, 2000]. Even assuming that the rifting of the supercontinent was initiated at ca. 850–900 Ma, as per [Timmons *et al.*, 2001], still for a timespan of more than 100 m.y. the continental Sr flux with high $^{87}\text{Sr}/^{86}\text{Sr}$ ratios must have maintained relatively high Sr ratios in sea water at the beginning of the Neo-Proterozoic. No such regularity, however, has been recorded in an express form. Apparently, the increase in continental Sr supply into the ocean was relatively short-lived and coincided with the culmination of the Grenville collisional events at ca. 1100 Ma, with a brief period of continental highstand. This corollary is in concert with the data on Precambrian rifting evolution [Khabarov, 2000]. The pre-Baikalian Late Riphean is an epoch of intensive growth of biogenic buildups. In major epicontinental basins of northern Eurasia, North America, China, and India, recorded is broad development of thick stromatolite bioherms and biostroms indicative of extensive continental flooding.

Sea-water Sr isotopic composition reflects global events

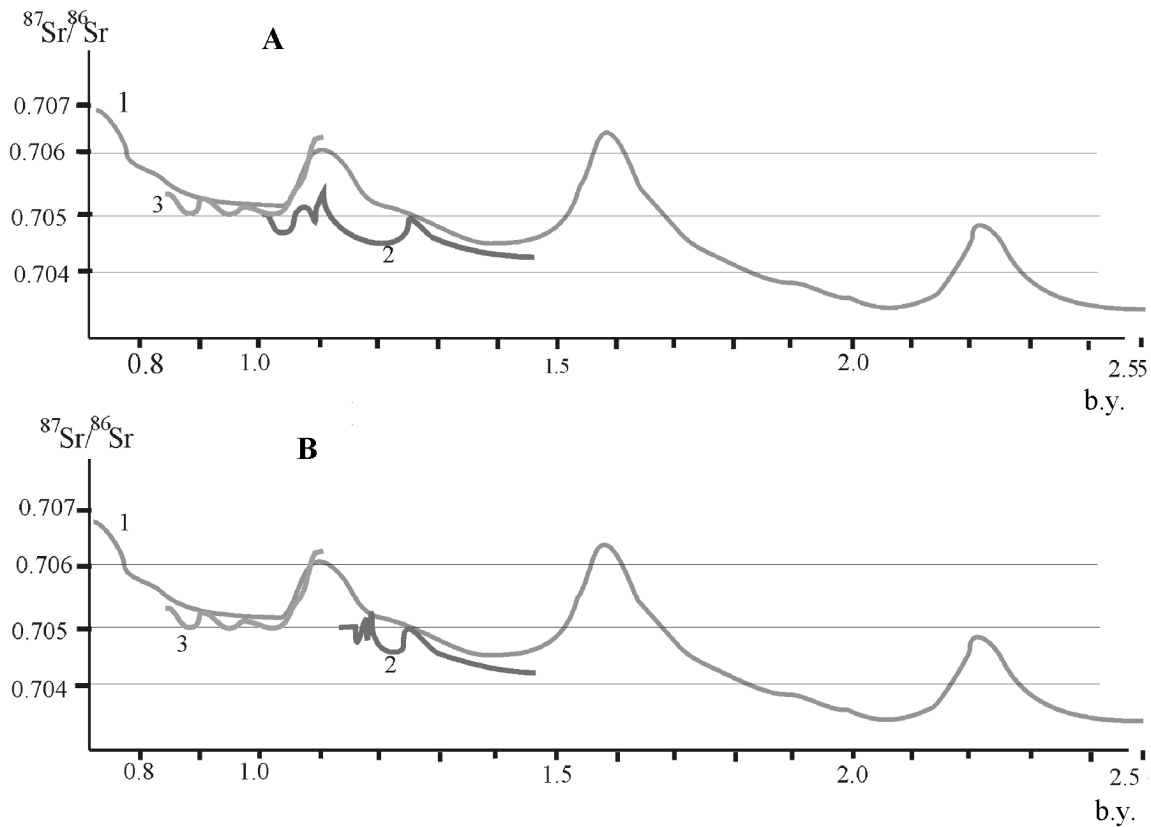


Figure 3. Variation curves of sea-water Sr isotopic composition in the Precambrian, (1) from published data [Asmerom *et al.*, 1991; Brasier and Lindsay, 1998; Derry and Jacobsen, 1988; Derry *et al.*, 1992; Faure, 1986; Gorokhov *et al.*, 1995, 1998; Hall and Veizer, 1996; Kuznetsov *et al.*, 1997, 2000; Mirota and Veizer, 1994; Pokrovsky and Vinogradov, 1991; Semikhatov *et al.*, 1998; Veizer *et al.*, 1992a, 1992b; Vinogradov *et al.*, 1998] and in the Baikit (2) and Yenisei (3) basins, Eastern Siberia. A and B, alternative options for chronological assignment of the $^{87}\text{Sr}/^{86}\text{Sr}$ curve for the Baikit basin.

in the upper geospheres; hence, time variations of $^{87}\text{Sr}/^{86}\text{Sr}$ ratios in the ocean are of interest not only to geodynamic reconstructions, but also for extracting the eustatic signal on relative sea-level variation curves, since changes in Sr isotope ratios are indirectly related to eustatic events [DePaola, 1986; Qing *et al.*, 1998].

Comparing $^{87}\text{Sr}/^{86}\text{Sr}$ trends and rock assemblages formed at different positions of the relative sea level (Figure 1) shows that in certain cases, lows on the $^{87}\text{Sr}/^{86}\text{Sr}$ curve correlate well with transgressions and relative sea-level highstands (the middle portion of the Yuktensky and lower parts of the Yurubchensky and Kuyumbinsky Sequences), while high Sr isotope ratios correspond to sea-level drops (the Dolgoktinsky and the lowermost Yuktensky Sequences). These data suggest that the most likely eustatic signal (in particular, sea-level drop) in sedimentary record of the Baikit basin is documented in Dolgoktinsky time (ca. 1250 Ma). These results correlate well with the $\delta^{13}\text{C}$ curve [Khabarov *et al.*, 2000, 2002].

Acknowledgments. This work was supported by the Russian Foundation for Basic Research (project no. 99-05-64671).

References

- Asmerom, Y., S. B. Jacobsen, A. H. Knoll, et al., Strontium isotopic variations of Neoproterozoic seawater: Implications for crustal evolution, *Geochim. Cosmochim. Acta.*, **55**, (10), 2883–2894, 1991.
- Bartley, J. K., M. A. Semikhatov, A. J. Kaufman, A. H. Knoll, M. C. Pope, and S. B. Jacobsen, Global events across the Mesoproterozoic–Neoproterozoic boundary: C and Sr isotopic evidence from Siberia, *Precamb. Res.*, **111**, (2), 165–202, 2001.
- Borg, G., The Koras–Sinclair–Ghanzi Rift in southern Africa. Volcanism, sedimentation, age relationship and geophysical signature of a late middle Proterozoic rift system, *Precamb. Res.*, **38**, (1), 75–90, 1988.
- Bozhko, N., Riphean accretion of terranes in the tectonic evolution of the Baikalian mountainous area (in Russian), *Dokl. Ross. Akad. Nauk*, **341**, (5), 654–657, 1995.
- Brand, U., and J. Veizer, Chemical diagenesis of a multicomponent carbonate system—II, Stable isotopes, *J. Sediment. Petrol.*, **51**, (3), 987–997, 1981.
- Brasier, M. D., and J. F. Lindsay, A billion years of environmental stability and emergence of eucariotes: new data from northern Australia, *Geology*, **26**, (6), 555–558, 1998.
- Bukharov, A., V. Khalilov, T. Strakhova, et al., Geology of the Baikal–Patom Upland: New evidence from U–Pb zircon dating (in Russian), *Geol. Geofiz.*, **12**, 29–40, 1992.
- Dalziel, I. W. D., Sh. Mosher, and L. M. Gahagan, Laurentia–

- Kalahari collision and the assembly of Rodinia, *J. Geol.*, **108**, (5), 499–513, 2000.
- DePaolo, D. J., Detailed record of the Neogene Sr isotopic evolution of seawater from DSDP Site 590B, *Geology*, **14**, (2), 103–106, 1986.
- Derry, L. A., and S. B. Jacobsen, The Nd and Sr evolution of Proterozoic seawater, *Geophys. Res. Lett.*, **15**, (4), 397–400, 1988.
- Derry, L. A., A. J. Kaufman, and S. B. Jacobsen, Sedimentary cycling and environmental change in the Late Proterozoic: Evidence from stable and radiogenic isotopes, *Geochim. Cosmochim. Acta.*, **56**, (3), 1317–1329, 1992.
- Dobretsov, N. L., and A. N. Bulgatov, *Geodynamic Map of Transbaikalia: Construction Principles and Legend*, 51 pp., Joint Institute of Geology, Geophysics, and Mineralogy, Siberian Division, Russian Academy of Sciences, Novosibirsk, 1991.
- Faure, G., *Principles of Isotope Geology*, 589 pp., Wiley, New York–Chichester–Brisbane–Toronto–Singapore, 1986.
- Gorokhov, I., M. Semikhatov, A. Baskakov, et al., Sr isotopic composition of Riphean, Vendian, and Lower Cambrian carbonate rocks (in Russian), *Stratigr. Geol. Korrelyatsiya*, **3**, (1), 3–33, 1995.
- Gorokhov, I., A. Kuznetsov, V. Melezhik, et al., Sr isotopic composition of Upper Jatulian dolomite of the Tulomozero Formation, southeastern Karelia (in Russian), *Dokl. Ross. Akad. Nauk*, **360**, (4), 609–612, 1998.
- Grotzinger, J. P., and J. F. Read, Evidence for primary aragonite precipitation, Lower Proterozoic (1.9 Ga) Rocknest dolomite, Wopmay orogen, Northwest Canada, *Geology*, **11**, (12), 710–713, 1983.
- Hall, S., and J. Veizer, Geochemistry of Precambrian carbonates: VII. Belt Supergroup, Montana and Idaho, USA, *Geochim. Cosmochim. Acta*, **60**, (4), 667–677, 1996.
- Khabarov, E. M., Evolution of rifting in the Precambrian, in *Issues of Sedimentology, Geochemistry, and Mineralization of Depositional Process* (abstract), 1st All-Russian Lithol. Conf., GEOS, Moscow, 349–354, 2000.
- Khabarov, E. M., V. A. Ponomarchuk, I. P. Morozova, et al., Carbon isotopes in carbonates of the western part of the Siberian craton and evolution of C isotope systems in Riphean basins, in *Geodynamics and Evolution of the Earth*, pp. 96–98, Scientific Research Center of the Joint Institute of Geology, Geophysics, and Mineralogy, Novosibirsk, 1996.
- Khabarov, E. M., I. P. Morozova, V. A. Ponomarchuk, et al., Correlation and age of petroliferous Riphean deposits of the Baikit anticline, Siberian craton: Isotope geochemical evidence (in Russian), *Dokl. Ross. Akad. Nauk*, **358**, (3), 378–380, 1998.
- Khabarov, E. M., V. A. Ponomarchuk, I. P. Morozova, and A. N. Travin, Carbon isotopes in Riphean carbonate rocks of the Yenisei Ridge (in Russian), *Stratigr. Geol. Korrelyatsiya*, **7**, (6), 20–40, 1999.
- Khabarov, E. M., V. A. Ponomarchuk, I. P. Morozova, I. V. Varaksina, and S. V. Saraev, Variations of sea level and C_{carb} isotopic composition in the Riphean basin of the western margin of the Siberian craton (Baikit anticline) (in Russian), *Geol. Geofiz.*, **43**, (3), 211–239, 2002.
- Khomentovskiy, V., and K. Nagovitsin, The Neo-Proterozoic of the west of the Siberian craton, *Geol. Geofiz.*, **39**, (10), 1365–1376, 1998.
- Knoll, A. N., A. J. Kaufman, and M. A. Semikhatov, The carbon-isotopic composition of Proterozoic carbonates: Riphean successions from northwestern Siberia (Anabar Massif, Turukhansk Uplift), *Am. J. Sci.*, **295**, (7), 823–850, 1995.
- Kontorovich, A. E., A. N. Izosimova, A. A. Kontorovich, et al., Geologic structure and conditions of formation of the vast Yurubcheno-Tokhomsky petroleum accumulation zone in the Upper Proterozoic of the Siberian craton (in Russian), *Geol. Geofiz.*, **37**, (8), 166–195, 1996.
- Kraevsky, B. G., and A. M. Pustylnikov, Structure and formative conditions of the Riphean deposits of the Katanga saddle, in *Methods Used in the Search for, and Conditions of Formation of Petroliferous Deposits of the Siberian Craton*, pp. 95–105, Siberian Research Institute of Geology, Geophysics, and Mineral Resources (SNIIGGIMS), Novosibirsk, 1991.
- Kuznetsov, A., I. Gorokhov, M. Semikhatov, et al., Sr isotopic composition in limestones of the Inzersky Formation, stratotypic for the Upper Riphean, South Urals (in Russian), *Dokl. Ross. Akad. Nauk*, **353**, (2), 249–254, 1997.
- Kuznetsov, A. B., I. M. Gorokhov, M. T. Krupenin, and R. Elmis, Stage-by-stage changes in Lower Riphean carbonate rocks of the Bakal ore field: Isotope geochemical evidence, in *Sedimentary Basins of the Urals and Adjacent Regions: Structural Regularities and Metallogeny*, pp. 106–111, Institute of Geology and Geochemistry, Ural Division, Russian Academy of Sciences, Yekaterinburg, 2000.
- McLelland, J., J. S. Daly, and J. M. McLelland, The Grenville Orogenic Cycle (ca. 1350–1000 Ma): an Adirondack perspective, *Tectonophysics*, **265**, (1), 1–28, 1996.
- Mirota, M. D., and J. Veizer, Geochemistry of Precambrian carbonates: VI. Aphebian Albanal Formations, Quebec, Canada, *Geochim. Cosmochim. Acta.*, **58**, (7), 1735–1745, 1994.
- Oliver, G. J. H., S. P. Johnson, I. S. Williams, and D. A. Herd, Relict 1.4 Ga oceanic crust in the Zambezi Valley, northern Zimbabwe: Evidence for Mesoproterozoic supercontinental fragmentation, *Geology*, **26**, (6), 571–573, 1998.
- Pokrovsky, B., and V. Vinogradov, Strontium, oxygen, and carbon isotopic composition in Upper Precambrian carbonates of the western slope of the Anabar uplift (the Kotuikan River) (in Russian), *Dokl. Akad. Nauk SSSR*, **320**, (5), 1245–1250, 1991.
- Ponomarchuk, V. A., and E. M. Khabarov, Meso-Proterozoic syn-depositional dolerites of the western part of the Siberian craton: Evidence for the breakup of Pangea I and formation of the Yenisei paleocean, in *Supercontinents in the Precambrian Geologic Evolution*, pp. 197–199, Proc. Conf., Irkutsk, June 4–6, 2001, Institute of the Earth's Crust, Siberian Division, Russian Academy of Sciences, 2001.
- Powell, C. M., Z. X. Li, M. W. McElhinny, et al., Paleomagnetic constraints on timing of the Neoproterozoic breakup of Rodinia and Cambrian formation of Gondwana, *Geology*, **21**, (10), 889–892, 1993.
- Qing, H., Ch. R. Barnes, D. Buhl, and J. Veizer, The strontium isotopic composition of Ordovician and Silurian brachiopods and conodonts: Relationships to geological events and implications for coeval seawater, *Geochim. Cosmochim. Acta*, **62**, (10), 1721–1733, 1998.
- Quick, J. E., Geology and origin of the Late Proterozoic Darb Zubaydah ophiolite, Kingdom of Saudi Arabia, *Bull. Geol. Soc. Am.*, **102**, (8), 1007–1020, 1990.
- Semikhatov, M., A methodological basis for stratigraphy of the Riphean (in Russian), *Stratigr. Geol. Korrelyatsiya*, **3**, (6), 33–50, 1995.
- Semikhatov, M., I. Gorokhov, A. Kuznetsov, et al., Sr isotopic composition of sea water in the initial Late Riphean: Limestones of the Lakhandinsky Group, Uchur–Maya region, Siberia (in Russian), *Dokl. Ross. Akad. Nauk*, **360**, (2), 236–240, 1998.
- Shenfil, V. Yu., *The Late Precambrian of the Siberian Craton*, 184 pp., Nauka, Novosibirsk, 1991.
- Sochava, A., V. Podkovyrov, and D. Vinogradov, Variations of C and O isotopic composition in carbonate rocks of the Vendian–Lower Cambrian of the Urinsky anticlinorium, southern Siberian craton (in Russian), *Litol. Polezn. Iskop.*, **3**, 279–289, 1996.
- Timmons, J. M., K. E. Karlstrom, C. M. Dehler, J. W. Geissman, and M. T. Heizler, Proterozoic multistage (ca. 1.1 and 0.8 Ga) extension recorded in the Grand Canyon Supergroup and establishment of northwest- and north-trending tectonic grains in the southwestern United States, *Bull. Geol. Soc. Am.*, **113**, (2), 163–180, 2001.
- Veizer, J., Trace elements and isotopes in sedimentary carbonates, in *Carbonates: Mineralogy and Geochemistry*, *Rev. Mineral.*, **11**, 265–300, 1983.
- Veizer, J., W. Compston, N. Clauer, and M. Schidlowski, $^{87}\text{Sr}/^{86}\text{Sr}$ in Late Proterozoic carbonates: Evidence for a “mantle” event at 900 Ma ago, *Geochim. Cosmochim. Acta*, **47**, (2), 295–302, 1983.

- Veizer, J., R. N. Clayton, and R. W. Hinton, Geochemistry of Precambrian carbonates: IV. Early Paleoproterozoic (2.25 ± 0.25 Ga) seawater, *Geochim. Cosmochim. Acta*, 56, (5), 875–885, 1992a.
- Veizer, J., K. A. Plumb, R. N. Clayton, et al., Geochemistry of Precambrian carbonates: V. Late Paleoproterozoic (1.8 ± 0.25 Ga) seawater, *Geochim. Cosmochim. Acta*, 56, (12), 2487–2501, 1992b.
- Vinogradov, V., B. Pokrovsky, A. Pustynnikov, et al., Isotope geochemical characteristics and age of Upper Precambrian deposits of the western part of the Siberian craton (in Russian), *Litol. Polezn. Iskop.*, 4, 49–75, 1994.
- Vinogradov, V., M. Korzh, I. Sorokina, et al., Isotopic evidence for epigenetic changes in pre-Vendian deposits of sedimentary cover on the Baikit uplift, Siberian craton (in Russian), *Litol. Polezn. Iskop.*, 3, 268–279, 1998.

(Received 9 July 2002)